Measurement of the decays $B_s^0 \to J/\psi\phi(1020)$, $B_s^0 \to J/\psi f_2'(1525)$ and $B_s^0 \to J/\psi K^+K^-$ at Belle

F. Thorne,[19] C. Schwanda,[19] I. Adachi,[13] H. Aihara,[58] D. M. Asner,[46] V. Aulchenko,[4] T. Aushev,[22] A. M. Bakich,[53] A. Bala,[47] B. Bhuyan,[16] G. Bonvicini,[63] M. Bračko,[31,23] M.-C. Chang,[8] V. Chekelian,[32] A. Chen,[38] B. G. Cheon,[11] K. Chilikin,[22] R. Chistov,[22] K. Cho,[26] V. Chobanova,[32] S.-K. Choi,[10] Y. Choi,[52] D. Cinabro,[63] J. Dalseno,[32,55] Z. Doležal,[5] Z. Drásal,[5] D. Dutta,[16] S. Eidelman,[4] S. Esen,[6] H. Farhat,[63] J. E. Fast,[46] M. Feindt,[25] T. Ferber,[7] V. Gaur,[54] N. Gabyshev,[4] R. Gillard,[63] R. Glattauer,[19] Y. M. Goh,[11] B. Golob,[30,23] J. Haba,[13] T. Hara,[13] K. Hayasaka,[36] H. Hayashii,[37] Y. Hoshi,[56] W.-S. Hou,[40] H. J. Hyun,[28] T. Iijima,[36,35] A. Ishikawa,[57] R. Itoh,[13] Y. Iwasaki,[13] T. Iwashita,[37] I. Jaegle,[12] T. Julius,[33] D. H. Kah,[28] J. H. Kang,[65] E. Kato,[57] C. Kiesling,[32] D. Y. Kim,[51] H. O. Kim,[28] J. B. Kim,[27] J. H. Kim,[26] M. J. Kim,[28] Y. J. Kim,[26] J. Klucar,[23] B. R. Ko,[27] P. Kodyš,[5] P. Križan,[30,23] P. Krokovny,[4] T. Kuhr,[25] J. S. Lange,[9] S.-H. Lee,[27] J. Libby,[17] C. Liu,[49] Y. Liu,[6] P. Lukin,[4] D. Matvienko,[4] H. Miyata,[43] R. Mizuk,[22,34] G. B. Mohanty,[54] A. Moll,[32,55] T. Mori,[35] Y. Nagasaka,[14] E. Nakano,[45] M. Nakao,[13] Z. Natkaniec,[41] M. Nayak,[17] C. Ng,[58] S. Nishida,[13] O. Nitoh,[60] S. Okuno,[24] C. Oswald,[3] G. Pakhlova,[22] H. Park,[28] H. K. Park,[28] R. Pestotnik,[23] M. Petrič,[23] L. E. Piilonen,[62] M. Prim,[25] M. Ritter,[32] A. Rostomyan,[7] S. Ryu,[50] H. Sahoo,[12] T. Saito,[57] Y. Sakai,[13] S. Sandilya,[54] L. Santelj,[23] T. Sanuki,[57] V. Savinov,[48] O. Schneider,[29] G. Schnell,[1,15] D. Semmler,[9] K. Senyo,[64] M. E. Sevior,[33] M. Shapkin,[20] C. P. Shen,[2] T.-A. Shibata,[59] J.-G. Shiu,[40] B. Shwartz,[4] A. Sibidanov,[53] F. Simon,[32,55] Y.-S. Sohn,[65] A. Sokolov,[20] E. Solovieva,[22] S. Stanič,[44] M. Starič,[23] U. Tamponi,[21,61] K. Tanida,[50] G. Tatishvili,[46] Y. Teramoto,[45] M. Uchida,[59] Y. Unno,[11] S. Uno,[13] P. Urquijo,[3] S. E. Vahsen,[12] G. Varner,[12] K. E. Varvell,[53] V. Vorobyev,[4] M. N. Wagner,[9] C. H. Wang,[39] M.-Z. Wang,[40] P. Wang,[18] X. L. Wang,[62] Y. Watanabe,[24] K. M. Williams,[62] E. Won,[27] J. Yamaoka,[12] Y. Yamashita,[42] S. Yashchenko,[7] C. Z. Yuan,[18] Z. P. Zhang,[49] V. Zhilich,[4] and A. Zupanc[25]

(Belle Collaboration)

[1]*University of the Basque Country UPV/EHU, 48080 Bilbao*
[2]*Beihang University, Beijing 100191*
[3]*University of Bonn, 53115 Bonn*
[4]*Budker Institute of Nuclear Physics SB RAS and Novosibirsk State University, Novosibirsk 630090*
[5]*Faculty of Mathematics and Physics, Charles University, 121 16 Prague*
[6]*University of Cincinnati, Cincinnati, Ohio 45221*
[7]*Deutsches Elektronen–Synchrotron, 22607 Hamburg*
[8]*Department of Physics, Fu Jen Catholic University, Taipei 24205*
[9]*Justus-Liebig-Universität Gießen, 35392 Gießen*
[10]*Gyeongsang National University, Chinju 660-701*
[11]*Hanyang University, Seoul 133-791*
[12]*University of Hawaii, Honolulu, Hawaii 96822*
[13]*High Energy Accelerator Research Organization (KEK), Tsukuba 305-0801*
[14]*Hiroshima Institute of Technology, Hiroshima 731-5193*
[15]*Ikerbasque, 48011 Bilbao*
[16]*Indian Institute of Technology Guwahati, Assam 781039*
[17]*Indian Institute of Technology Madras, Chennai 600036*
[18]*Institute of High Energy Physics, Chinese Academy of Sciences, Beijing 100049*
[19]*Institute of High Energy Physics, Vienna 1050*
[20]*Institute for High Energy Physics, Protvino 142281*
[21]*INFN-Sezione di Torino, 10125 Torino*
[22]*Institute for Theoretical and Experimental Physics, Moscow 117218*
[23]*Jozef Stefan Institute, 1000 Ljubljana*
[24]*Kanagawa University, Yokohama 221-8686*
[25]*Institut für Experimentelle Kernphysik, Karlsruher Institut für Technologie, 76131 Karlsruhe*
[26]*Korea Institute of Science and Technology Information, Daejeon 305-806*
[27]*Korea University, Seoul 136-713*
[28]*Kyungpook National University, Daegu 702-701*
[29]*École Polytechnique Fédérale de Lausanne (EPFL), Lausanne 1015*
[30]*Faculty of Mathematics and Physics, University of Ljubljana, 1000 Ljubljana*
[31]*University of Maribor, 2000 Maribor*
[32]*Max-Planck-Institut für Physik, 80805 München*

[33]School of Physics, University of Melbourne, Victoria 3010
[34]Moscow Physical Engineering Institute, Moscow 115409
[35]Graduate School of Science, Nagoya University, Nagoya 464-8602
[36]Kobayashi-Maskawa Institute, Nagoya University, Nagoya 464-8602
[37]Nara Women's University, Nara 630-8506
[38]National Central University, Chung-li 32054
[39]National United University, Miao Li 36003
[40]Department of Physics, National Taiwan University, Taipei 10617
[41]Henryk Niewodniczanski Institute of Nuclear Physics, Krakow 31-342
[42]Nippon Dental University, Niigata 951-8580
[43]Niigata University, Niigata 950-2181
[44]University of Nova Gorica, 5000 Nova Gorica
[45]Osaka City University, Osaka 558-8585
[46]Pacific Northwest National Laboratory, Richland, Washington 99352
[47]Panjab University, Chandigarh 160014
[48]University of Pittsburgh, Pittsburgh, Pennsylvania 15260
[49]University of Science and Technology of China, Hefei 230026
[50]Seoul National University, Seoul 151-742
[51]Soongsil University, Seoul 156-743
[52]Sungkyunkwan University, Suwon 440-746
[53]School of Physics, University of Sydney, New South Wales 2006
[54]Tata Institute of Fundamental Research, Mumbai 400005
[55]Excellence Cluster Universe, Technische Universität München, 85748 Garching
[56]Tohoku Gakuin University, Tagajo 985-8537
[57]Tohoku University, Sendai 980-8578
[58]Department of Physics, University of Tokyo, Tokyo 113-0033
[59]Tokyo Institute of Technology, Tokyo 152-8550
[60]Tokyo University of Agriculture and Technology, Tokyo 184-8588
[61]University of Torino, 10124 Torino
[62]CNP, Virginia Polytechnic Institute and State University, Blacksburg, Virginia 24061
[63]Wayne State University, Detroit, Michigan 48202
[64]Yamagata University, Yamagata 990-8560
[65]Yonsei University, Seoul 120-749

(Received 3 September 2013; published 2 December 2013)

We report a measurement of the branching fraction of the decay $B_s^0 \to J/\psi\,\phi(1020)$, evidence and a branching fraction measurement for $B_s^0 \to J/\psi f_2'(1525)$, and the determination of the total $B_s^0 \to J/\psi K^+K^-$ branching fraction, including the resonant and nonresonant contributions to the K^+K^- channel. We also determine the S-wave contribution within the $\phi(1020)$ mass region. The absolute branching fractions are $\mathcal{B}[B_s^0 \to J/\psi\,\phi(1020)] = (1.25 \pm 0.07(\mathrm{stat}) \pm 0.08(\mathrm{syst}) \pm 0.22(f_s)) \times 10^{-3}$, $\mathcal{B}[B_s^0 \to J/\psi f_2'(1525)] = (0.26 \pm 0.06(\mathrm{stat}) \pm 0.02(\mathrm{syst}) \pm 0.05(f_s)) \times 10^{-3}$, and $\mathcal{B}[B_s^0 \to J/\psi K^+K^-] = (1.01 \pm 0.09(\mathrm{stat}) \pm 0.10(\mathrm{syst}) \pm 0.18(f_s)) \times 10^{-3}$, where the last systematic error is due to the branching fraction of $b\bar{b} \to B_s^{(*)}\bar{B}_s^{(*)}$. The branching fraction ratio is found to be $\mathcal{B}[B_s^0 \to J/\psi f_2'(1525)]/\mathcal{B}[B_s^0 \to J/\psi\,\phi(1020)] = (21.5 \pm 4.9(\mathrm{stat}) \pm 2.6(\mathrm{syst}))\%$. All results are based on a 121.4 fb^{-1} data sample collected at the $\Upsilon(5S)$ resonance by the Belle experiment at the KEKB asymmetric-energy e^+e^- collider.

DOI: 10.1103/PhysRevD.88.114006 PACS numbers: 13.25.Hw, 14.40.Nd

I. INTRODUCTION

The study of $B_s^0\bar{B}_s^0$ mixing and CP violation in B_s^0 decays [1] helps advance our understanding of the Cabibbo-Kobayashi-Maskawa mechanism [2,3]. The decay $B_s^0 \to J/\psi\,\phi(1020)$ [4] probes the CP-violating phase ϕ_s of $B_s^0\bar{B}_s^0$ oscillations [5–8], which is predicted to be small within the standard model (SM). However, contributions from physics beyond the SM can significantly enhance this parameter [9].

In this context, experiments have made significant progress to better understand contributions to the decay $B_s^0 \to J/\psi K^+K^-$ beyond $B_s^0 \to J/\psi\,\phi(1020)(\to K^+K^-)$. A recent discovery in this field is the decay $B_s^0 \to J/\psi f_2'(1525)$, whose branching fraction relative to $B_s^0 \to J/\psi\,\phi(1020)$ is measured to be $(26.4 \pm 2.7(\mathrm{stat}) \pm 2.4(\mathrm{syst}))\%$ by LHCb [10] and $(19 \pm 5(\mathrm{stat}) \pm 4(\mathrm{syst}))\%$ by DØ [11]. A first measurement of the entire $B_s^0 \to J/\psi K^+K^-$ decay rate (including resonant and nonresonant decays) was recently performed by LHCb with a measured branching fraction of $(7.70 \pm 0.08(\text{stat}) \pm 0.39(\text{syst}) \pm 0.60(f_s/f_d)) \times 10^{-4}$ [12].

In this analysis, we study the decay $B_s^0 \to J/\psi K^+K^-$ using the Belle data and determine its absolute branching fraction. We identify the resonant contributions $B_s^0 \to J/\psi \phi(1020)(\to K^+K^-)$ and $B_s^0 \to J/\psi f_2'(1525)(\to K^+K^-)$ and determine the S-wave contribution in the $\phi(1020)$ mass region. In contrast to hadron collider experiments, we normalize to the absolute number of $B_s^0\bar{B}_s^0$ pairs produced rather than to a reference decay channel. In addition, to determine the S-wave contribution in the $\phi(1020)$ mass region, we fit to the K^+K^- mass distribution rather than perform an angular analysis. Thus, our results are obtained using methods with systematic uncertainties that both differ from previous analyses.

II. EXPERIMENTAL PROCEDURE

A. Data sample and event selection

The data used in this analysis were taken with the Belle detector [13] at the KEKB asymmetric-energy e^+e^- collider [14]. Belle is a large-solid-angle magnetic spectrometer that consists of a silicon vertex detector, a 50-layer central drift chamber (CDC), an array of aerogel threshold Cherenkov counters (ACC), a barrel-like arrangement of time-of-flight (TOF) scintillation counters, and an electromagnetic calorimeter (ECL) comprised of CsI(Tl) crystals located inside a superconducting solenoid coil that provides a 1.5 T magnetic field. An iron flux return located outside of the coil is instrumented to detect K_L^0 mesons (KLM) and to identify muons.

The Belle data sample taken at the $\Upsilon(5S)$ resonance has an integrated luminosity of 121.4 fb^{-1} and contains $(7.1 \pm 1.3) \times 10^6$ $B_s^0\bar{B}_s^0$ events with a cross section for the process $e^+e^- \to b\bar{b}$ of $\sigma_{b\bar{b}} = (0.340 \pm 0.016)$ nb and a fraction of $b\bar{b}$ states hadronizing into $B_s^{(*)}\bar{B}_s^{(*)}$ of $f_s = (17.2 \pm 3.0)\%$ [15].

Monte Carlo (MC) simulated events equivalent to at least 6 times the integrated luminosity of the data are used to evaluate the signal acceptance and perform background studies. MC events are generated with EVTGEN [16], and a full detector simulation based on GEANT3 [17] is applied. QED bremsstrahlung is included using the PHOTOS package [18].

Hadronic events are selected based on the charged track multiplicity and the visible energy in the calorimeter. Charged tracks are required to originate from within 4 cm along the beam axis and 0.5 cm in the transverse plane with respect to the e^+e^- interaction point. Electron candidates are identified using the ratio of the energy detected in the ECL to the track momentum, the ECL shower shape, position matching between the track and ECL cluster, the energy loss in the CDC (dE/dx), and the response of the ACC counters. Muons are identified based on their penetration range and transverse scattering in the KLM detector. Kaon candidates are distinguished from pion tracks by using combined information from the CDC, the ACC, and the TOF scintillation counters.

To reconstruct J/ψ mesons, two identified leptons with the same flavor (e or μ) and opposite charges are combined. The energy loss from bremsstrahlung is partially recovered by adding back the four-momentum of any photon within a 5° cone around the electron or positron direction. The invariant masses of the $J/\psi \to e^+e^-(\gamma)$ and $J/\psi \to \mu^+\mu^-$ candidates are required to lie within the range $2.946\ \text{GeV} < M(e^+e^-(\gamma)) < 3.133\ \text{GeV}$ and $3.036\ \text{GeV} < M(\mu^+\mu^-) < 3.133\ \text{GeV}$, respectively. The J/ψ mass resolution is approximately 11 MeV in the electron channel and about 10 MeV in the muon channel. Asymmetric mass windows are used to accommodate the residual bremsstrahlung tails.

The J/ψ candidate is combined with two oppositely charged kaon candidates to form a B_s^0 candidate. We accept candidates in the entire K^+K^- phase space. The resolution in $M(K^+K^-)$ is approximately 1 MeV. Due to the two-body kinematics in the process $e^+e^- \to \Upsilon(5S) \to B_s^{(*)}\bar{B}_s^{(*)}$, the B_s^0 signal is extracted using the following two kinematic variables: the energy difference $\Delta E = E_B^* - E_{\text{beam}}^*$ and the beam-energy constrained mass $M_{\text{bc}} = \sqrt{E_{\text{beam}}^{*2} - (\vec{p}_B^{\,*})^2}$, where E_{beam}^* is the beam energy in the center-of-mass (c.m.) frame of the colliding beams, and E_B^* and $\vec{p}_B^{\,*}$ denote the energy and the momentum of the reconstructed B_s^0 meson, respectively, in the c.m. system. As the photon from the decay $B_s^* \to B_s^0\gamma$ is not reconstructed, there are three signal regions in the $(M_{\text{bc}}, \Delta E)$ plane, corresponding to the three initial states $B_s^0\bar{B}_s^0$, $B_s^0\bar{B}_s^*$ (or $B_s^*\bar{B}_s^0$), and $B_s^*\bar{B}_s^*$. We select the most abundant initial state $B_s^*\bar{B}_s^*$ [the $B_s^*\bar{B}_s^*$ fraction in $B_s^{(*)}\bar{B}_s^{(*)}$ events being $f_{B_s^*\bar{B}_s^*} = (87.0 \pm 1.7)\%$ [15]] by requiring $-0.2\ \text{GeV} < \Delta E < 0.1\ \text{GeV}$ and $M_{\text{bc}} > 5.4\ \text{GeV}$, as the signal peaks around $\Delta E = M(B_s^*) - M(B_s^0) \approx 0.049\ \text{GeV}$ and $M_{\text{bc}} = M(B_s^*) \approx 5.415\ \text{GeV}$ for the $B_s^*\bar{B}_s^*$ signal region.

B. Backgrounds and signal extraction

Background to the $B_s^0 \to J/\psi K^+K^-$ signal arises from random combinations in $\Upsilon(5S)$ events and from so-called continuum, i.e., events originating from the process $e^+e^- \to q\bar{q}$ with $q = u$, d, s, or c. Contributions from the latter are suppressed by exploiting the difference in event shape between $\Upsilon(5S)$ and continuum events (spherical vs jetlike, respectively) and requiring the ratio of the second to zeroth Fox-Wolfram moment $R_2 = H_2/H_0$ [19] to be less than 0.4. This selection was optimized for this decay topology in the analysis of the decay $B_s^0 \to J/\psi\pi^+\pi^-$ [20].

Signal extraction is performed independently for the $J/\psi \to e^+e^-$ and $J/\psi \to \mu^+\mu^-$ subsamples by a two-dimensional unbinned maximum likelihood fit in ΔE and $M(K^+K^-)$. The fit range is $-0.2\ \text{GeV} < \Delta E < 0.1\ \text{GeV}$

and $0.95\ \text{GeV} < M(K^+K^-) < 2.4\ \text{GeV}$ and takes into account resolution effects at the lower end of the $M(K^+K^-)$ phase space. The probability density function (PDF) for signal [21] in ΔE is parametrized with a sum of a Gaussian and a Crystal Ball [22] function (a sum of two Gaussian functions) for the $J/\psi \to e^+e^-$ ($J/\psi \to \mu^+\mu^-$) data sample. The parameters of these PDFs are determined from data using a control sample of $B^0 \to J/\psi K^*(892)^0$ decays with $K^*(892)^0 \to K^+\pi^-$. The signal shapes of the $\phi(1020)$ and the $f_2'(1525)$ resonances in $M(K^+K^-)$ are each described by a nonrelativistic Breit-Wigner function whose width includes both the natural width and the detector resolution. The remaining $J/\psi(K^+K^-)_{\text{other}}$ component is modeled with an ARGUS function [23] in $M(K^+K^-)$. When we perform the fit on the data, the shape parameters of all signal PDFs for the ΔE distribution are fixed using the control sample, while the parameters of the signal PDFs for the $M(K^+K^-)$ distribution are fixed using MC simulations.

The background, which includes contributions from combinatorial background in $\Upsilon(5S)$ events and continuum background, is parametrized by a first-order polynomial in ΔE and an ARGUS function in $M(K^+K^-)$. The parameters of the background PDFs are determined from a data sideband defined by $5.25\ \text{GeV} < M_{\text{bc}} < 5.35\ \text{GeV}$ and fixed in the fit on the real data.

The entire signal extraction procedure has been tested and validated on simulated events. Terms in the PDF due to interference among the $J/\psi\phi(1020)$, $J/\psi f_2'(1525)$, and $J/\psi(K^+K^-)_{\text{other}}$ components cancel after integration over angular variables, since the K^+K^- systems have distinct quantum numbers of 1, 2, and 0, respectively. As we find that the angular acceptance is approximately flat within our statistics, we do not consider interference effects among these components.

The yields obtained for the $J/\psi \to e^+e^-$ and $J/\psi \to \mu^+\mu^-$ samples are given in Table I. Figures 1 and 2 show the projections of the fit in ΔE and $M(K^+K^-)$, respectively.

III. RESULTS AND SYSTEMATIC UNCERTAINTIES

The absolute branching fraction for the decay $B_s^0 \to J/\psi\phi(1020)$ is calculated from the fitted yields in Table I as

$$\mathcal{B}[B_s^0 \to J/\psi\phi(1020)] = \frac{N_{J/\psi\phi(1020)}}{2\mathcal{L}\sigma_{b\bar{b}} f_s f_{B_s^*\bar{B}_s^*}\epsilon\mathcal{B}[J/\psi \to \ell^+\ell^-]\mathcal{B}[\phi(1020) \to K^+K^-]}, \quad (1)$$

where $N_{J/\psi\phi(1020)}$ is the extracted yield, $\mathcal{L}$ is the luminosity of the Belle $\Upsilon(5S)$ sample, and $\mathcal{B}[J/\psi \to \ell^+\ell^-]$ and $\mathcal{B}[\phi(1020) \to K^+K^-]$ are the subdecay branching fractions. The parameter ϵ denotes the reconstruction efficiency, whose values are given in Table II. Applying this formula to the electron and muon samples and averaging the results, we obtain

TABLE I. Extracted yields for signal components and background in the $J/\psi \to e^+e^-$ and $J/\psi \to \mu^+\mu^-$ samples.

Channel	e^+e^-	$\mu^+\mu^-$
$J/\psi\phi(1020)$	168 ± 13.5	158 ± 13
$J/\psi f_2'(1525)$	34 ± 10	26 ± 8
$J/\psi(K^+K^-)_{\text{other}}$	83 ± 17	67 ± 14
Background	232 ± 19	300 ± 20

$$\mathcal{B}[B_s^0 \to J/\psi\phi(1020)] = (1.25 \pm 0.07(\text{stat}) \pm 0.08(\text{syst}) \pm 0.22(f_s)) \times 10^{-3}, \quad (2)$$

where the first uncertainty is statistical, the second is systematic, and the third is due to the uncertainty in f_s. Similarly, we obtain for $B_s^0 \to J/\psi f_2'(1525)$

$$\mathcal{B}[B_s^0 \to J/\psi f_2'(1525)] = (0.26 \pm 0.06(\text{stat}) \pm 0.02(\text{syst}) \pm 0.05(f_s)) \times 10^{-3}. \quad (3)$$

The branching fraction ratio is

$$\frac{\mathcal{B}[B_s^0 \to J/\psi f_2'(1525)]}{\mathcal{B}[B_s^0 \to J/\psi\phi(1020)]} = (21.5 \pm 4.9(\text{stat}) \pm 2.6(\text{syst}))\%. \quad (4)$$

The significance of the $B_s^0 \to J/\psi f_2'(1525)$ signal is equal to 3.3 standard deviations (including the systematic uncertainty), which is calculated from the difference of the log-likelihood values of the default fit and a fit including background components only.

The branching fraction for the entire $B_s^0 \to J/\psi K^+K^-$ component [including the nonresonant decay and the resonant contributions $B_s^0 \to J/\psi\phi(1020)$ and $B_s^0 \to J/\psi f_2'(1525)$] is

$$\mathcal{B}[B_s^0 \to J/\psi K^+K^-] = (1.01 \pm 0.09(\text{stat}) \pm 0.10(\text{syst}) \pm 0.18(f_s)) \times 10^{-3}. \quad (5)$$

The contributions to the systematic uncertainties given in Eqs. (2)–(5) are listed in Table III and fall into three categories: uncertainties in the input parameters in Eq. (1), uncertainties related to signal and detector response simulation, and the PDF model. The first class

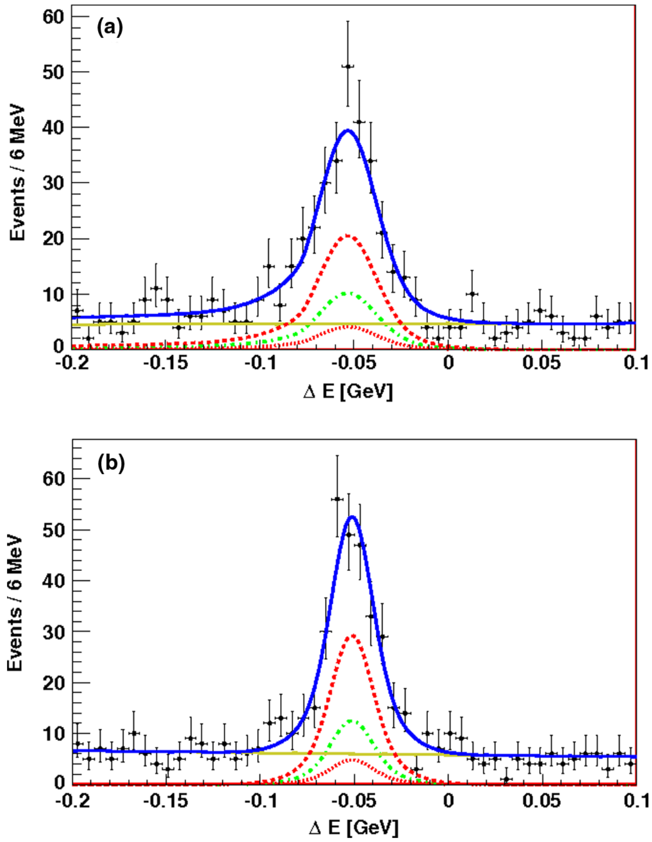

FIG. 1 (color online). Projection of the fit in ΔE for (a) $J/\psi \to e^+e^-$ and (b) $J/\psi \to \mu^+\mu^-$ events. The black points with error bars are the data and the upper solid line corresponds to the entire PDF model. From top to bottom, the peaking components are $J/\psi\phi(1020)$, $J/\psi(K^+K^-)_{\mathrm{other}}$, and $J/\psi f_2'(1525)$. Background is shown by the lower solid line.

of uncertainties is dominant because of the large uncertainty in f_s, which we quote separately.

To estimate the error related to the $\phi(1020)$ polarization in the simulation of $B_s^0 \to J/\psi\phi(1020)$, we use the difference in efficiency between a simulation using the polarization parameters determined by CDF [5] and a different sample giving equal weights to each helicity amplitude.

The systematic error related to lepton ($\ell^\pm$) identification is determined using $\gamma\gamma \to \ell^+\ell^-$ events. The uncertainty arising from kaon identification is determined from a sample of $D^{*+} \to D^0\pi^+$, $D^0 \to K^-\pi^+$ decays.

The error related to the PDF parameters is obtained by performing 1000 pseudoexperiments, sampling each parameter from a Gaussian distribution having a mean value and width equal to the parameter's central value and uncertainty. The width of the distribution of signal yields is taken as the systematic uncertainty. As we do not find significant impact from the correlations among the parameters, we sample each parameter independently when performing this calculation.

The systematic error due to the PDF model is estimated by repeating the fit with alternative PDF functions,

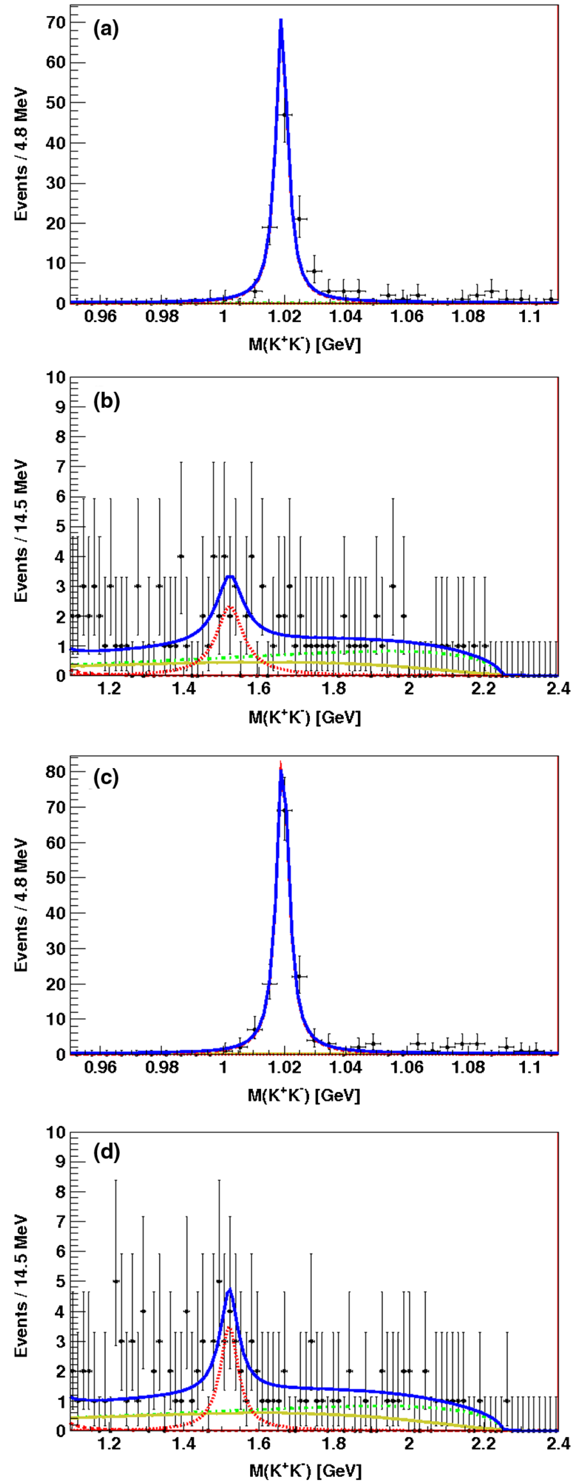

FIG. 2 (color online). Projection of the fit in $M(K^+K^-)$ for events in the signal range -0.07 GeV $< \Delta E < -0.03$ GeV. Panels (a) and (b) show the $\phi(1020)$ and $f_2'(1525)$ mass regions, respectively, for $J/\psi \to e^+e^-$ events; panels (c) and (d) are the same for $J/\psi \to \mu^+\mu^-$ events. In all plots, the upper solid line corresponds to the entire PDF model, which overlaps with the curve of the $J/\psi\phi(1020)$ component in (a) and (c). The signal components and the background are shown using the line style of Fig. 1.

TABLE II. Reconstruction efficiency ϵ for all three investigated decay modes. The quoted error corresponds to the uncertainty due to the MC statistics.

Channel	$\epsilon_{e^+e^-}$[%]	$\epsilon_{\mu^+\mu^-}$[%]
$J/\psi\phi(1020)$	31.0 ± 0.1	33.2 ± 0.1
$J/\psi f_2'(1525)$	28.4 ± 0.2	30.5 ± 0.2
$J/\psi(K^+K^-)_{\rm other}$	29.7 ± 0.1	32.5 ± 0.1

including a relativistic Breit-Wigner function and a nonrelativistic Breit-Wigner function with a phase space correction for the $\phi(1020)$ and $f_2'(1525)$ resonances, and a pure phase space description for the $J/\psi(K^+K^-)_{\rm other}$ component. The maximum deviation between these fit results and the results obtained with the default model is taken as a systematic uncertainty. Only for the $J/\psi(K^+K^-)_{\rm other}$ component was a significant deviation found. For the $J/\psi\phi(1020)$ and the $J/\psi f_2'(1525)$ components the deviations were negligibly small.

The total systematic error is calculated separately for the electron and muon channels by adding all components in quadrature. For the calculation of the weighted mean value, the systematic errors are treated as fully correlated.

As an additional result, the S-wave contribution in the $\phi(1020)$ mass region is calculated using the signal yields presented in Table I. Here, we assume that the K^+K^- system in $B_s^0 \to J/\psi(K^+K^-)_{\rm other}$ is a pure S wave. This assumption is supported by the observed helicity angle distribution of $J/\psi(K^+K^-)_{\rm other}$, where the helicity angle is defined as the angle between the K^+ meson and the B_s^0 meson in the K^+K^- rest frame. Hence, the S-wave fraction (S) is the fitted yield of $J/\psi(K^+K^-)_{\rm other}$ events relative to the yield of $J/\psi K^+K^-$ within a specific mass range,

TABLE III. Contribution to the systematic uncertainty in the $B_s^0 \to J/\psi K^+K^-$ branching fractions.

Source	Uncertainty [%]
Luminosity	0.7
$\sigma_{b\bar{b}}$ [15]	4.7
f_s [15]	17.4
$f_{B_s^*\bar{B}_s^*}$ ($B_s^*\bar{B}_s^*$ fraction in $B_s^{(*)}\bar{B}_s^{(*)}$)	2.0
$\mathcal{B}[J/\psi \to \ell^+\ell^-]$ [24]	1.0
$\mathcal{B}[\phi(1020) \to K^+K^-]$ [24]	1.0
$\mathcal{B}[f_2'(1525) \to K^+K^-]$ [24]	2.5
MC statistics	0.3–0.8
$\phi(1020)$ polarization	1.3
Charged tracking	1.4
Electron identification	3.1
Muon identification	3.0
Kaon identification	1.9
PDF parameters:	
$J/\psi_{e^+e^-}\phi(1020)$	1.1
$J/\psi_{\mu^+\mu^-}\phi(1020)$	1.0
$J/\psi_{e^+e^-}(K^+K^-)_{\rm other}$	9.1
$J/\psi_{\mu^+\mu^-}(K^+K^-)_{\rm other}$	5.8
$J/\psi_{e^+e^-}f_2'(1525)$	7.8
$J/\psi_{\mu^+\mu^-}f_2'(1525)$	5.4
PDF model:	
$J/\psi_{e^+e^-}(K^+K^-)_{\rm other}$	2.4
$J/\psi_{\mu^+\mu^-}(K^+K^-)_{\rm other}$	3.0

TABLE IV. The $J/\psi K^+K^-$ S-wave contribution in different mass regions around the $\phi(1020)$ resonance. The first error is statistical, the second systematic, and the third error is the uncertainty due to a possible $B_s^0 \to J/\psi f_0(980)$ contribution.

Mass range	1.009–1.028 GeV
CDF [5]	$(0.8 \pm 0.2)\%$
This analysis	$(0.47 \pm 0.07 \pm 0.22^{+2.2}_{-0})\%$
Mass range	1.007–1.031 GeV
LHCb [12]	$(1.1 \pm 0.1^{+0.2}_{-0.1})\%$
This analysis	$(0.57 \pm 0.09 \pm 0.26^{+2.0}_{-0})\%$

$$S = \frac{\alpha N[J/\psi(K^+K^-)_{\rm other}]}{\alpha N[J/\psi(K^+K^-)_{\rm other}] + \beta N[J/\psi\phi(1020)]}, \quad (6)$$

where α and β denote the fractions of $J/\psi(K^+K^-)_{\rm other}$ and $J/\psi\phi(1020)$, respectively, within the mass range considered. $N[J/\psi(K^+K^-)_{\rm other}]$ and $N[J/\psi\phi(1020)]$ are the fitted yields from Table I. The results are shown in Table IV for the mass ranges used in hadron collider experiments. While the statistical uncertainty is propagated via the fitted yields, the systematic uncertainty in the S-wave contribution due to the PDF parametrization uncertainties and the PDF model are propagated through α and β.

To estimate the systematic uncertainty due to a possible $B_s^0 \to J/\psi f_0(980)$ contribution, as seen, e.g., by LHCb [12], we investigate the difference between the PDF model used in this analysis and the PDF model used by LHCb, which describes the $B_s^0 \to J/\psi f_0(980)$ component with a Flatté function in $M(K^+K^-)$. From the S-wave contribution of 1.1% obtained by LHCb, we calculate the value of the parameter α in the LHCb PDF model. We find an increase in α from 0.8% (1.0%) to 5.0% for the CDF (LHCb) mass range in the electron channel, and from 0.9% (1.1%) to 5.0% in the muon channel. We assign this variation as an additional model uncertainty, which we quote separately in Table IV.

IV. SUMMARY

In summary, we present a measurement of the absolute branching fraction for the decay $B_s^0 \to J/\psi\phi(1020)$ [Eq. (2)]. This result is in good agreement with the CDF

Run I result [24,25] as well as their preliminary results based on the full data sample [26] and the current LHCb result [12]. We obtain evidence for the decay $B_s^0 \to J/\psi f_2'(1525)$ [Eqs. (3) and (4)], in good agreement with the measurements by LHCb [10,12] and DØ [11]. We also present a measurement of the entire $B_s^0 \to J/\psi K^+ K^-$ component including resonant and nonresonant decays [Eq. (5)]. Finally, we determine the S-wave fraction of $B_s^0 \to J/\psi K^+ K^-$ in the $\phi(1020)$ mass region (Table IV). Our central value is somewhat lower than the LHCb and CDF values but in agreement with their results when including the systematic error due to a possible $B_s^0 \to J/\psi f_0(980)$ component.

ACKNOWLEDGMENTS

We thank the KEKB group for the excellent operation of the accelerator; the KEK cryogenics group for the efficient operation of the solenoid, and the KEK computer group, the National Institute of Informatics, and the PNNL/EMSL computing group for valuable computing and SINET4 network support. We acknowledge support from the Ministry of Education, Culture, Sports, Science, and Technology (MEXT) of Japan, the Japan Society for the Promotion of Science (JSPS), and the Tau-Lepton Physics Research Center of Nagoya University; the Australian Research Council and the Australian Department of Industry, Innovation, Science and Research; Austrian Science Fund under Grant No. P 22742-N16; the National Natural Science Foundation of China under Contracts No. 10575109, No. 10775142, No. 10875115, and No. 10825524; the Ministry of Education, Youth and Sports of the Czech Republic under Contract No. MSM0021620859; the Carl Zeiss Foundation, the Deutsche Forschungsgemeinschaft and the VolkswagenStiftung; the Department of Science and Technology of India; the Istituto Nazionale di Fisica Nucleare of Italy; The BK21 and WCU program of the Ministry Education Science and Technology, National Research Foundation of Korea Grants No. 2010-0021174, No. 2011-0029457, No. 2012-0008143, No. 2012R1A1A2008330, BRL program under NRF Grant No. KRF-2011-0020333, and GSDC of the Korea Institute of Science and Technology Information; the Polish Ministry of Science and Higher Education and the National Science Center; the Ministry of Education and Science of the Russian Federation and the Russian Federal Agency for Atomic Energy; the Slovenian Research Agency; the Basque Foundation for Science (IKERBASQUE) and the UPV/EHU under program UFI 11/55; the Swiss National Science Foundation; the National Science Council and the Ministry of Education of Taiwan; and the U.S. Department of Energy and the National Science Foundation. This work is supported by a Grant-in-Aid from MEXT for Science Research in a Priority Area ("New Development of Flavor Physics"), and from JSPS for Creative Scientific Research ("Evolution of Tau-lepton Physics").

---

[1] I. Dunietz, R. Fleischer, and U. Nierste, Phys. Rev. D **63**, 114015 (2001).
[2] M. Kobayashi and T. Maskawa, Prog. Theor. Phys. **49**, 652 (1973).
[3] N. Cabibbo, Phys. Rev. Lett. **10**, 531 (1963).
[4] Throughout this paper, the inclusion of the charge-conjugate decay mode is implied.
[5] T. Aaltonen *et al.* (CDF Collaboration), Phys. Rev. Lett. **109**, 171802 (2012).
[6] V. M. Abazov *et al.* (DØ Collaboration), Phys. Rev. D **85**, 032006 (2012).
[7] R. Aaij *et al.* (LHCb Collaboration), Phys. Rev. D **87**, 112010 (2013).
[8] G. Aad *et al.* (ATLAS Collaboration), J. High Energy Phys. 12 (2012) 072.
[9] K. Anikeev *et al.*, FERMILAB Report No. 01-197, 2001, and references therein.
[10] R. Aaij *et al.* (LHCb Collaboration), Phys. Rev. Lett. **108**, 151801 (2012).
[11] V. M. Abazov *et al.* (DØ Collaboration), Phys. Rev. D **86**, 092011 (2012).
[12] R. Aaij *et al.* (LHCb Collaboration), Phys. Rev. D **87**, 072004 (2013).
[13] A. Abashian *et al.* (Belle Collaboration), Nucl. Instrum. Methods Phys. Res., Sect. A **479**, 117 (2002); also see detector section in J. Brodzicka *et al.*, Prog. Theor. Exp. Phys. **2012**, 04D001 (2012).
[14] S. Kurokawa and E. Kikutani, Nucl. Instrum. Methods Phys. Res., Sect. A **499**, 1 (2003), and other papers included in this volume; T. Abe *et al.*, Prog. Theor. Exp. Phys. **2013**, 03A001 (2013), and following articles up to 03A011.
[15] S. Esen *et al.* (Belle Collaboration), Phys. Rev. D **87**, 031101 (2013).
[16] D. J. Lange, Nucl. Instrum. Methods Phys. Res., Sect. A **462**, 152 (2001).
[17] R. Brun, F. Bruyant, M. Maire, A. C. McPherson, and P. Zanarini, Report No. CERN-DD/EE/84-1, 1984.
[18] E. Barberio and Z. Was, Comput. Phys. Commun. **79**, 291 (1994).
[19] G. C. Fox and S. Wolfram, Phys. Rev. Lett. **41**, 1581 (1978).
[20] J. Li *et al.* (Belle Collaboration), Phys. Rev. Lett. **106**, 121802 (2011).
[21] In this paper, "signal" refers to all of $B_s^0 \to J/\psi \phi(1020)(\to K^+K^-)$, $B_s^0 \to J/\psi f_2'(1525)(\to K^+K^-)$, and $B_s^0 \to J/\psi (K^+K^-)_{\rm other}$. The notation $J/\psi (K^+K^-)_{\rm other}$ includes the nonresonant decay $B_s^0 \to J/\psi K^+ K^-$ as well

as decays via resonant intermediate states, except the $\phi(1020)$ and the $f_2'(1525)$ resonance.

[22] T. Skwarnicki, Ph.D. thesis, Institute for Nuclear Physics, Krakow, 1986; DESY Internal Report No. DESY F31-86-02, 1986.

[23] H. Albrecht *et al.* (ARGUS Collaboration), Phys. Lett. B **241**, 278 (1990).

[24] J. Beringer *et al.* (Particle Data Group) Phys. Rev. D **86**, 010001 (2012), and 2013 partial update for the 2014 version.

[25] F. Abe *et al.* (CDF Collaboration), Phys. Rev. D **54**, 6596 (1996).

[26] O. Norniella, K. Pitts *et al.* CDF Collaboration, Public Note No. 10795, 2012.